Available online at www.sciencedirect.com

SciVerse ScienceDirect

Geochimica et Cosmochimica Acta 85 (2012) 326–341

Geochimica et Cosmochimica Acta

www.elsevier.com/locate/gca

Influence of humic acid imposed changes of ferrihydrite aggregation on microbial Fe(III) reduction

Katja Amstaetter [a,1], Thomas Borch [b], Andreas Kappler [a,*]

[a] Geomicrobiology, Center for Applied Geosciences, University of Tübingen, Sigwartstrasse 10, D-72076 Tübingen, Germany
[b] Department of Soil and Crop Sciences and Department of Chemistry, Colorado State University, Fort Collins, CO 80523, USA

Received 27 July 2011; accepted in revised form 1 February 2012; available online 21 February 2012

Abstract

Microbial reduction of Fe(III) minerals at neutral pH is faced by the problem of electron transfer from the cells to the solid-phase electron acceptor and is thought to require either direct cell-mineral contact, the presence of Fe(III)-chelators or the presence of electron shuttles, e.g. dissolved or solid-phase humic substances (HS). In this study we investigated to which extent the ratio of Pahokee Peat Humic Acids (HA) to ferrihydrite in the presence and absence of phosphate influences rates of Fe(III) reduction by *Shewanella oneidensis* MR-1 and the identity of the minerals formed. We found that phosphate generally decreased reduction rates by sorption to the ferrihydrite and surface site blocking. In the presence of low ferrihydrite concentrations (5 mM), the addition of HA helped to overcome this inhibiting effect by functioning as electron shuttle between cells and the ferrihydrite. In contrast, at high ferrihydrite concentrations (30 mM), the addition of HA did not lead to an increase but rather to a decrease in reduction rates. Confocal laser scanning microscopy images and ferrihydrite sedimentation behaviour suggest that the extent of ferrihydrite surface coating by HA influences the aggregation of the ferrihydrite particles and thereby their accessibility for Fe(III)-reducing bacteria. We further conclude that in presence of dissolved HA, iron reduction is stimulated through electron shuttling while in the presence of only sorbed HA, no stimulation by electron shuttling takes place. In presence of phosphate the stimulation effect did not occur until a minimum concentration of 10 mg/l of dissolved HA was reached followed by increasing Fe(III) reduction rates up to dissolved HA concentrations of approximately 240 mg/l above which the electron shuttling effect ceased. Not only Fe(III) reduction rates but also the mineral products changed in the presence of HA. Sequential extraction, XRD and ^{57}Fe-Mössbauer spectroscopy showed that crystallinity and grain size of the magnetite produced by Fe(III) reduction in the presence of HA is lower than the magnetite produced in the absence of HA. In summary, this study shows that both the concentration of HA and Fe(III) minerals strongly influence microbial Fe(III) reduction rates and the mineralogy of the reduction products. Thus, deviations in iron (hydr)oxide reactivity with changes in aggregation state, such as HA induced ferrihydrite aggregation, need to be considered within natural environments.

1. INTRODUCTION

Fe(II) and Fe(III) minerals such as siderite ($Fe^{II}CO_3$), vivianite ($Fe^{II}_3(PO_4)_2 * 8H_2O$), magnetite ($Fe^{II}Fe^{III}_2O_4$), ferrihydrite ($Fe^{III}(OH)_3$), goethite ($\alpha$-$Fe^{III}OOH$), lepidocrocite ($\gamma$-$Fe^{III}OOH$) or hematite ($\gamma - Fe^{III}_2O_3$) are subject to a large number of chemical and biological redox transformations in the environment. The biologically driven iron redox cycle includes Fe(III)-reducing as well as Fe(II)-oxidizing bacteria that inhabit a broad range of environments including, oxic, anoxic, microoxic, pH-neutral or acidic, ambient-temperature and hydrothermal conditions (Lovley et al., 2004; Kappler and Straub, 2005; Weber et al., 2006; Konhauser et al., 2011). Members of the genera *Shewanella*

* Corresponding author. Fax: +49 7071 295059.
E-mail address: andreas.kappler@uni-tuebingen.de (A. Kappler).
[1] Present address: CDM Consult GmbH, Neue Bergstrasse 13, D-64665 Alsbach, Germany.

0016-7037/$ - see front matter © 2012 Elsevier Ltd. All rights reserved.
http://dx.doi.org/10.1016/j.gca.2012.02.003

and *Geobacter* have been found to be the dominating species in pH-neutral environments promoting microbial iron reduction (Thamdrup, 2000; Lovley et al., 2004).

In order to use poorly soluble iron (oxyhydr)oxides as terminal electron acceptor which cannot pass the cell membrane, iron-reducing microorganisms have developed at least three different strategies to transfer electrons: Electron transfer (1) by direct contact between cells and the mineral surface, (2) by reduction of complexed and thus solubilized Fe(III) facilitated by endogenous or exogenous chelating compounds, and (3) by using redox-active electron shuttling molecules (for review see Lovley et al., 2004; Lovley, 2008). Electron transfer via direct contact between cells and the mineral surface has been suggested to be mediated via conductive pili or pilus-like appendages (Reguera et al., 2005; Gorby et al., 2006) and via outer membrane cytochromes (Ruebush et al., 2006). However, there is substantial evidence that microbial Fe(III) reduction does not necessarily need direct contact between cells and minerals (Nevin and Lovley, 2002b; Lies et al., 2005). Flavin compounds, capable of electron shuttling and Fe(III) complexation, were shown to be produced and excreted by *Shewanella* strains (Taillefert et al., 2007; Marsili et al., 2008; von Canstein et al., 2008).

Besides these relatively simple and structurally defined organic molecules, heterogeneous humic substances (HS) can stimulate Fe(III) mineral reduction (Lovley et al., 1996b). HS are common constituents of soils and sediments, composed of detrital organic material containing metal-ion-complexing and redox-active functional groups (Stevenson, 1994). HS can be separated into three fractions with different pH dependent water solubility (i.e., fulvic acids, humic acids (HA), and humins). 9,10-anthraquinone-2,6-disulfonate (AQDS) has often been used in laboratory studies as a simple surrogate for quinone moieties in HS (Coates et al., 1998; Fredrickson et al., 1998; Kukkadapu et al., 2004; O'Loughlin, 2008). However, the significance of experiments in which HS are substituted by artificial electron shuttling compounds such as AQDS for understanding microbial electron transfer and mineral transformation is questionable due to the heterogeneous, polymeric and polydispersive nature of HS. For instance, in contrast to AQDS (Wolf et al., 2009), HS strongly sorb to Fe minerals and show a pH-dependent solubility behaviour. The structure of HS is also known to vary with geochemical conditions such as pH, ionic strength and HS redox state. Thus, the availability of redox active functional groups is likely to change as a function of molecule aggregation (Thieme et al., 2007).

It has been suggested that HS can stimulate microbial iron reduction in three ways: (1) by solubilization of Fe(III) minerals via iron complexation and transport of the Fe(III) to the cells (Lovley et al., 1996a; Nevin and Lovley, 2002a), (2) by complexation of Fe(II), thus preventing surface site blockage and providing thermodynamically favourable conditions for Fe(III) reduction (Royer et al., 2002b), or (3) via electron shuttling by transferring electrons from the cells to the Fe(III) minerals (Lovley et al., 1996b; Royer et al., 2002a; Bauer and Kappler, 2009). Studies investigating electron shuttling typically have been conducted using very high HS concentrations (up to 2 g/l) (Lovley et al., 1996b; Coates et al., 1998), compared to natural concentrations of HS between 0.4 mg/l in groundwater and 60 mg/l in surface water (Aiken, 1985) (0.2–30 mg C/l). Recently it has been shown that electron shuttling between cells and ferrihydrite occurs if the dissolved HA concentration exceeds a minimum of 5 mg C/l (Jiang and Kappler, 2008). The stimulation by HA ceased at a maximum reduction rate for HA concentrations of 25 mg C/l and higher (Jiang and Kappler, 2008). All these studies exclusively describe the effect of dissolved HS on microbial iron reduction. Recently, it has been shown that also solid-phase humic compounds can function as electron shuttles (Roden et al., 2010). Additionally, it can be expected that sorption of HS to iron mineral surfaces (Weng et al., 2006; Kaiser et al., 2007) will influence the reactivity of these iron minerals (Mikutta and Kretzschmar, 2008) and the bacteria-mineral interactions, respectively. The charge and accessibility of the mineral surface was shown to change after sorption of organic polymers (Kretzschmar and Sticher, 1997; Mikutta et al., 2008). However, the effect of dissolved versus sorbed HS on the function of HS as electron shuttle and on the microbial transformation of iron minerals has not been determined.

The identity and properties of the mineral products formed during microbial iron reduction are of interest because of their ability to release, transform and sequester nutrients or pollutants (Borch et al., 2010). The formation of specific mineral phases during microbial iron reduction does not depend on a specific microbial strain but rather on the geochemical conditions present during their formation (Mann, 2001; Konhauser et al., 2008; Piepenbrock et al., 2011). Previous studies showed a slow Fe(II)-induced recrystallization (via a reductive dissolution-reprecipitation or structural rearrangement mechanism) of ferrihydrite to goethite, lepidocrocite or hematite at low Fe(II) concentrations at the mineral surface (Gálvez et al., 1999; Cornell and Schwertmann, 2003) while elevated Fe(II) concentrations lead to magnetite formation by topotactic conversion of the ferrihydrite (Ardizzone and Formaro, 1983). Consequently, depending on Fe(II) concentration, lepidocrocite (Fredrickson et al., 2003), goethite and magnetite (Hansel et al., 2003; Kukkadapu et al., 2004; Borch et al., 2007) have been identified as products of microbial Fe(III) reduction. The amount of Fe(II) present during the reduction process and the rate of Fe(II) formation controls the transformation of ferrihydrite to either goethite or magnetite (Zachara et al., 2002; Coker et al., 2008). Additionally, the presence of bicarbonate or phosphate during microbial iron reduction either leads to preferential formation of siderite (Fredrickson et al., 1998) or green rust and vivianite (Hansel et al., 2003; Borch et al., 2007), depending on the concentration of these anions. The different iron phases produced during microbial Fe(III) reduction differ in redox reactivity and sorption capacity. Therefore, identification of the geochemical factors controlling the type and reactivity of the secondary iron minerals formed is essential for prediction of pollutant degradation and nutrient sequestration (Borch et al., 2010). The effect of HS on the identity of biogenic iron minerals formed during Fe(III) reduction has not been determined systematically so far.

In summary, the effects of HS at naturally relevant concentrations on microbial iron reduction are poorly understood. Based on the knowledge outlined above we hypothesize that the HA concentration influences the microbial reducibility of ferrihydrite as well as the identity of the minerals produced during microbial reduction. Therefore the main objectives of this study were: (1) to determine the range of HA concentrations that lead to stimulation of microbial ferrihydrite reduction, (2) to identify and evaluate the effects of dissolved versus adsorbed HA on ferrihydrite reduction, and (3) to identify the biogenic precipitates formed during ferrihydrite reduction in presence of phosphate and HA.

2. EXPERIMENTAL PROCEDURES

2.1. Bacterial cultures

Shewanella oneidensis strain MR-1 was kindly provided by Jeff Gralnick (Univ. Minnesota). We chose this strain as our model strain since it is well characterized, easy to cultivate and for its ability to utilize a broad variety of different substrates (Nealson and Myers, 1990; Venkateswaran et al., 1999). Aerobic cultures on lysogeny broth (Luria Bertani medium; LB medium) agar plates were streaked out from a frozen stock kept at −80 °C. LB-medium contained (per l): 10 g tryptone, 5 g yeast extract and 5 g NaCl (for LB-plates 12 g agar was added). LB-plates were incubated at 28 °C for approximately 24 h and afterwards kept at 4 °C for up to 10 days. For liquid cultures, 50 ml of liquid LB medium in a 200 ml Erlenmeyer flask were inoculated with a single colony from the LB-plate. The capped flask was incubated at 28 °C on a rotary shaker at 150 rpm under initial oxic conditions. The cell concentration in LB-cultures was determined by optical density (OD) measurements at 600 nm. OD_{600} was calibrated against cell counts obtained by direct counting with a Thoma-chamber by light microscopy (Axioscope 2, Zeiss, Germany). At the end of exponential growth, cells had consumed O_2 completely and switched to anaerobic metabolism (Lies et al., 2005). The inoculum for experiments was prepared as follows: 2 ml of a LB-grown cell culture was harvested after 14 h at late exponential growth phase and centrifuged (5 min, 10,600 g). Cells were washed twice with LML medium, resuspended in 2 ml of medium and diluted to a final concentration of 2×10^5 cells/ml in culture tubes containing LML medium. LML medium was prepared after Myers and Myers (1994), containing 12 mM HEPES buffer (pH 7) and 30 mM lactate as electron donor. The pH was adjusted with NaOH instead of $NaHCO_3$ before autoclaving.

2.2. Preparation of ferrihydrite suspensions and humic substance solutions

Ferrihydrite was synthesized according to Schwertmann and Cornell (2000) and Raven et al. (1998) by adding 40 g of $Fe(NO_3)_3 * 9H_2O$ to 500 ml water followed by pH adjustment (1 M KOH) to a final pH of 7.2. After centrifugation and 4 times washing with Millipore®-water, the wet pellet was resuspended in water to an approximate concentration of 0.5 M Fe(III). This suspension was stored in the dark in tightly closed serum bottles (butyl rubber stoppers). Deoxygenation under vigorous stirring was done by alternating application of vacuum and N_2 purging for 10 min each in total three times. The freeze-dried mineral product was characterized by μ-X-ray diffraction (μ-XRD). Since we observed the formation of crystalline mineral phases (hematite) either after autoclaving or after storing the ferrihydrite suspension for longer than 3 months (Fig. A1, Appendix 1 in Supplementary data), suspensions used for this study were not sterilized and always used within 2 months after synthesis for experiments. N_2-BET measurements of several independently synthesized batches of the ferrihydrite yielded surface areas between 240–280 m^2/g after freeze-drying.

For experiments with HA, IHSS (International Humic Substances Society) Pahokee Peat Humic Acid 1R103H2 was dissolved either in Millipore®-water or 50 mM phosphate buffer (pH 7) at different concentrations of up to 24 mg/ml following previous studies (e.g. Jiang and Kappler, 2008). If necessary, the pH was readjusted to 7 by dropwise addition of 2 M NaOH. The HA solutions were shaken for 1 h before filter-sterilization (cellulose acetate, 0.2 μm) into autoclaved culture tubes closed with butyl rubber stoppers. After filtration the solution was deoxygenated under sterile conditions by alternating application of vacuum and N_2 for 5 min each.

2.3. Experimental setup

Fe(III) reduction experiments were conducted in LML medium with 30 mM lactate as electron donor. To monitor Fe(II) and mineral formation during microbial Fe(III) reduction, approximately 30 tubes were set up per experimental condition in parallel with the same amount of medium, ferrihydrite, cells, phosphate or HA, respectively (for a complete list of experimental setups see Table A1, Appendix 2 in Supplementary data). Sterile culture tubes (total volume 23 ml) were filled with 9 ml (cultures containing 5 mM i.e. 0.5 g/l ferrihydrite) or 6 ml (cultures containing 30 mM i.e. 3.2 g/l ferrihydrite) of anoxic LML-medium. The headspace was exchanged with N_2 and the tubes were sealed with butyl rubber stoppers. For sample treatments in the glove box (mineral preparation, sequential extraction) smaller culture tubes with screw cap fixed butyl rubber stoppers (total volume 17 ml) were used. Finally, ferrihydrite suspension, HA solution (prepared either in water or phosphate buffer, see above) or phosphate buffer solution, and the cells (final cell number: 2×10^5 cells/ml) were injected with syringes and the tubes were incubated horizontally at 28 °C in the dark. In experiments where phosphate buffer or HA dissolved in phosphate buffer was added, the final phosphate concentration was 0.8 mM.

At each sampling time, several tubes (from the 30 parallel tubes) were selected (1) to quantify total Fe(II) and total Fe(III) concentrations by acid digestion and (2) to obtain samples for mineral identification by ^{57}Fe-Mössbauer spectroscopy and XRD and for sequential extraction of iron minerals. Complete digestion of the biogenic solids in the tubes was necessary in order to avoid inhomogeneous sampling with syringes and to determine the total amount of Fe(II)

and Fe(III) including precipitates that sorbed to the glass walls. In order to calculate the maximum reduction rates, these total Fe(II) concentrations were plotted against time. A linear regression was used to derive the maximum slope for Fe(III) reduction rates during exponential phase (for examples see Fig. A2, Appendix 3 in Supplementary data).

Nearly all experiments were performed at least twice. The reduction rates of replicate experiments were used to calculate average values of iron reduction rates for one specific experimental condition. The experiment with 400 mg/l HA and phosphate and a few of the phosphate-free experiments were performed once, but three parallel tubes were analyzed to determine the total Fe(II) concentration at each sampling time point. Total iron concentrations were usually slightly lower than aimed for (3.8–4.8 mM instead of 5 mM, 24–29 mM instead of 30 mM) due to variations of the concentration in ferrihydrite stocks and due to dilution by adding the various solutions (HA, etc.) but will be referred to as 5 and 30 mM ferrihydrite setups throughout the text.

Our experiments included setups that contained combinations of medium, cells or ferrihydrite both in the presence or absence of phosphate without any HA amendments (Table A1, Appendix 2 in Supplementary data). The reduction rates determined for those experiments therefore also account for potential effects of endogenous shuttling compounds excreted by the bacteria. In the absence of bacteria, no iron reduction was observed.

2.4. Sampling

In order to determine total concentrations of Fe(III) and Fe(II) (see below), culture tubes were sacrificed at different time points and the minerals in the tubes were completely dissolved by adding 2.25 and 3 ml of 12 M HCl to the 5 and 30 mM ferrihydrite cultures, respectively.

Samples for ^{57}Fe-Mössbauer spectroscopy, μ-XRD and sequential extraction were prepared in an anoxic glove box (100% N_2 atmosphere) harvesting one screw-cap culture tube for each analysis at the chosen time-point. The samples were transferred stepwise into 2 ml-Eppendorf® tubes and centrifuged (2 min, 9700 g). Subsamples of the supernatant were kept in the glove box and analyzed for dissolved Fe(II) and Fe(tot). The remaining solids were prepared for ^{57}Fe-Mössbauer spectroscopy, dried for μ-XRD or sequentially extracted. It has to be noted that after the initial centrifugation step, not only dissolved Fe^{2+} but also small ferrihydrite colloids with sorbed Fe(II) could be present in the supernatant. However, based on the absence of significant concentrations of dissolved Fe(III) (see e.g. Fig. 7), we consider this fraction to be negligible.

2.5. Sequential extraction

The protocol for sequential iron mineral extraction was modified after Roden and Zachara (1996). Loosely bound Fe(II) was extracted by a 1 M sodium acetate solution (pH 5). Vivianite and poorly crystalline minerals such as ferrihydrite were dissolved in 0.5 M HCl, whereas crystalline minerals such as goethite, magnetite and hematite were dissolved in 6 M HCl. Control experiments showed that synthetic siderite was dissolved partly in the acetate extraction solution and completely dissolved in 0.5 M HCl (data not shown).

Solutions used for the extraction steps under anoxic conditions were purged with N_2 (30 min) before being brought into the glove box. For the first extraction step, 1.5 ml anoxic sodium acetate solution was added to the precipitates (that were separated by centrifugation) and incubated for 24 h in the dark. The mixture was centrifuged (2 min, 9700*g*) and the supernatant was kept for Fe analysis. The residual solid was extracted with 1.5 ml of anoxic 0.5 M HCl. After 2 h of incubation (in the dark), the mixture was again centrifuged and the supernatant was kept for Fe analysis. The remaining solids were dissolved in 1.5 ml of 6 M HCl at 70 °C in a water bath for 30 min outside the glove box. The extract was then analyzed for the Fe content.

2.6. Analytical methods

Dissolved HA were quantified by absorption measurements at 465 nm with a plate reader of filtered samples (Spin-X nylon membrane tubes, 0.22 μm, Costar, USA). LML-medium or phosphate buffer did not show significant interference at this wavelength. A filtered stock solution of IHSS standard Pahokee Peat Humic Acid (1R103H2) was diluted in 50 mM phosphate buffer to obtain a calibration curve between 0.03 and 0.3 g/l. It is known that sorption of HA to the ferrihydrite surface is not homogeneous for all HA molecules present and leads to a slight fractionation of HA (Sharma et al., 2010). However, Sharma and coworkers (2010) showed that this does not cause significant variations in calculation of the actual HA concentrations. Additionally, due to the high concentration of non-humic organic molecules stemming from the microbial growth medium, quantification of HA via alternative methods such as DOC analysis was not possible.

Fe(II) was quantified using the ferrozine assay (Stookey, 1970). In order to quantify total iron (Fe(tot)) concentrations, aliquots were reduced with 10% w/v $NH_2OH * HCl$ dissolved in 1 M HCl. Fe(II) and Fe(tot) samples were mixed with a 0.1% (w/v) solution of ferrozine prepared in 50% (w/v) ammonium acetate buffer. Absorbance was measured at 562 nm in microtiter plates with a plate reader. It has been shown previously that even high concentrations of natural organic matter do not interfere with the ferrozine assay (Voillier et al., 2000).

Samples taken right after setting up the cultures showed that iron concentrations in the filtrates (present due to complexation by humic substances) or dispersed ferrihydrite particles were below or close to the detection limit of the ferrozine assay, even at high HA concentrations. Only after 3 weeks, concentrations of approximately 0.1 mM of Fe(III) were detectable in the filtrate of cell-free setups containing 0.6 g/l HA and 5 mM ferrihydrite suggesting the formation of HA-Fe colloids or complexes with a size less than 0.45 μm.

The specific surface area of iron minerals was determined by the Brunauer-Emmett-Teller (BET) method with a Gemini 2375 Surface Area Analyzer (Micromeritics, Germany) with N_2 as adsorbing gas. Dry mineral samples

were degassed for 30 min under vacuum at 105 °C, before measuring a five-point-BET-curve.

Microscopic analysis was performed at a Leica TCS SP2 confocal laser scanning microscope. Cells were stained using the NanoOrange protein dye (Invitrogen, USA) in a 1:100 dilution. Excitation wavelength of the laser was set to 458–514 nm (max. 485 nm) and fluorescence of the protein dye was detected between 530 and 630 nm (max. 590 nm). Three different sections of each sample were scanned along the z-axis to collect light microscopy and fluorescent data simultaneously at different focus levels.

For ^{57}Fe-Mössbauer spectroscopic analysis (the instrument was set to detect exclusively ^{57}Fe species and will be named Mössbauer spectroscopy throughout the script) wet mineral samples were sealed between layers of Kapton® tape in the anoxic glove box. Samples were mounted in a close-cycle exchange-gas cryostat (Janis, USA) that allowed cooling of the sample to 4.2 K. Mössbauer spectra were collected with a constant acceleration drive system in transmission mode and with a ^{57}Co source. Spectra were calibrated against a spectrum of alpha-Fe metal foil collected at room temperature. Spectra calibration and fitting was performed with Recoil software (University of Ottawa, Canada) using Voigt based spectral lines.

For μ-XRD analyses, dried precipitates were prepared in the anoxic glove box. The solids were grinded in an agate mortar, suspended in approximately 50 μl of N_2-flushed ethanol and transferred with a glass pipette into small indentations (diameter 2 mm) on a silicon wafer. After evaporation of the ethanol, the samples were covered in the anoxic glovebox with a piece of clear plastic wrap (polyethylene) which remained oxygen tight for approximately 45 min (based on tests with chemically synthesized Fe(II) carbonate minerals, not shown) and allowed XRD analysis outside the glovebox under anoxic conditions. The μ-XRD-device (Bruker D8 Discover X-ray diffraction instrument, Bruker AXS GmbH, Germany) consists of a Co K_α X-ray tube, operating at 30 kV, 30 mA, which is either connected to a polycapillary that allows measurements at a spot diameter of 50 μm or a monocapillary with a spot diameter of 300 μm. Each sample was measured in three overlapping frames of 30° 2θ, within 1 min measuring time for each frame, using a GADDS® area detector. The EVA® 10.0.1.0 software was used to merge the three measured frames of one sample and to identify the contained mineral phases using the PDF-database licensed by ICDD (International Centre for Diffraction Data). X-ray diffractograms showed a broad signal in a 2θ range from 17° to 29°, originating from the polyethylene foil which was used to protect the samples from oxidation. In this range and at smaller angels the intensity of the X-rays diffracted by the mineral lattice is reduced, due to the foil.

3. RESULTS AND DISCUSSION

3.1. Effect of phosphate and HA on Fe(III) reduction rates and extent

To determine the influence of HA on microbial reduction of ferrihydrite and mineral transformation, IHSS standard Pahokee Peat Humic Acid was added at different concentrations to cultures of *Shewanella oneidensis* MR-1 containing either 5 mM (0.53 mg/l) or 30 mM (3.21 mg/l) ferrihydrite. Since phosphate is environmentally relevant and can influence microbial reduction and specifically its mineral products (Fredrickson et al., 1998; Zachara et al., 2002; Borch et al., 2007), we also determined the effect of phosphate on Fe(III) reduction rates and mineral transformation.

Phosphate binds strongly to iron oxide surfaces and has been shown to hinder microbial Fe(III) reduction (Borch et al., 2007). Although we observed a decrease in reduction rates in the presence of 0.8 mM phosphate in both 5 and 30 mM ferrihydrite setups (Fig. 1), we did not detect a significant change in the percentage of Fe(III) reduced at the end of microbial reduction, compared to phosphate-free setups. The extent of Fe(III) reduction reached up to 80–90% within 4–8 days in all 5 mM ferrihydrite setups and was thus almost complete. Approximately 40% of Fe(III) were reduced in the 30 mM ferrihydrite setups within 5–11 days. This is in contrast to the study by Borch et al. (2007), where Fe(II) formation decreased with increasing phosphate concentration (although in that study complete ferrihydrite reduction was not observed even in absence of phosphate). However, in their study microbial reduction was most likely not finished at the time point of analysis (after 7 days). Some of the differences observed could also be due to the different medium composition (HEPES buffer and 30 mM lactate in our study vs. PIPES buffer and 3 mM lactate in the study by Borch and co-authors) and due to the different Fe(III) mineral substrates (pure ferrihydrite in our study vs. ferrihydrite-coated quartz sand, see e.g. differences observed by Ekstrom et al., 2010).

In our study, the reduction rates decreased for both ferrihydrite concentrations (5 and 30 mM) in the presence of phosphate but the reduction extent remained constant (Fig. 1). Differences in Fe(III) reduction rates in the presence of phosphate were also previously described by Fredrickson et al. (1998) who compared reduction of 45 mM hydrous ferric oxide (HFO) by *Shewanella putrefaciens* CN32 in either bicarbonate- or PIPES-buffered medium, both with and without 4 mM phosphate. They found that in the first three days of microbial iron reduction phosphate slowed down the reduction process in PIPES-buffered medium (with 27 mM lactate), comparable to our observations in HEPES-buffered medium (with 30 mM lactate). In contrast, in presence of bicarbonate buffer Fredrickson and co-workers (1998) observed similar Fe(III) reduction rates with and without phosphate.

The addition of HA did also not change the extent of reduction in our experiments but instead it increased the rate of Fe(III) reduction under certain conditions (Fig. 1). At the low ferrihydrite concentration (5 mM), stimulation of iron reduction by HA (compared to the HA-free but phosphate-containing setups) was observed at total HA concentrations ranging from 50 to 400 mg/l, although at 400 mg/l HA, iron reduction rates did not further increase compared to the 200 mg/l setup (Fig. 1c). In contrast, at 30 mM ferrihydrite only a HA concentration of 50 mg/l caused stimulation of ferrihydrite reduction (Fig. 1d). At HA concentrations above 50 mg/l, the reduction rates decreased to values even

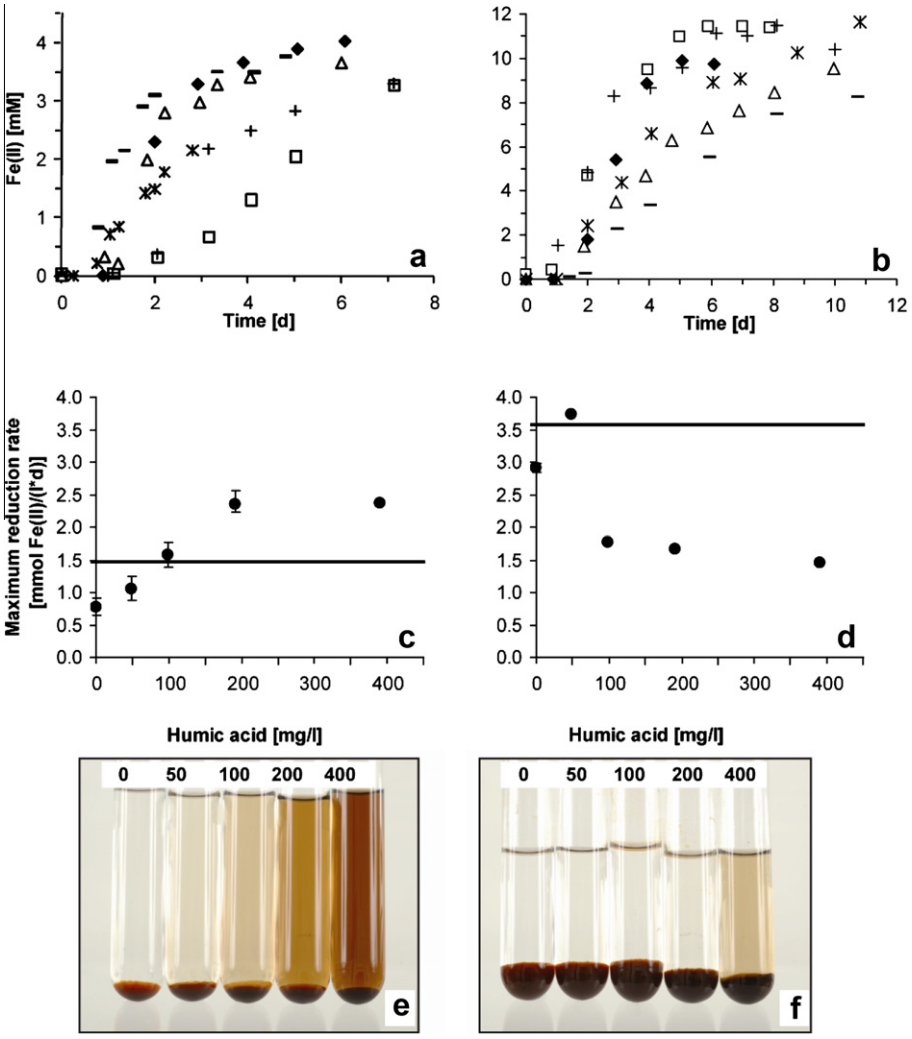

Fig. 1. Total Fe(II) formed over time by *Shewanella oneidensis* MR-1 in cultures containing (a) 5 mM and (b) 30 mM ferrihydrite with no additions (♦), 0.8 mM phosphate (□), 50 mg/l HA (+), 100 mg/l HA (∗), 200 mg/l HA (△) and 400 mg/l HA (−) (all cultures amended with HA contained 0.8 mM phosphate), representative experiments are shown (please note the differing scales in panel a and b). Maximum rates for microbial reduction of (c) 5 mM and (d) 30 mM ferrihydrite by *Shewanella oneidensis* MR-1 in cultures containing different total concentrations of HA and in all cases 0.8 mM phosphate. Solid horizontal lines indicate maximum reduction rates of cultures that contained neither phosphate nor HA. Error bars indicate highest and lowest values for the maximum rate obtained from replicate experiments. In panel d error bars are smaller than the symbols. Images of culture supernatants after addition of different concentrations of HA, in the presence of (e) 5 mM and (f) 30 mM ferrihydrite. Pictures show, from left to right, tubes containing 0, 50, 100, 200 and 400 mg/l HA (total concentrations; all tubes contain 0.8 mM phosphate). All images were taken before microbial Fe(III) reduction started.

lower than the rate determined in presence of only phosphate, probably by blocking of ferrihydrite surface sites by HA. At all HA concentrations tested, the Fe(III) reduction rates in 30 mM ferrihydrite setups did not significantly exceed the reduction rates measured in absence of phosphate. These results show a strong dependence of microbial iron reduction rates on the ratio of HA to ferrihydrite and will be discussed in detail in section 3.2 and 3.4.

3.2. Microbial electron transfer in presence of dissolved and sorbed HA

The acceleration of Fe(III) reduction observed in some of our experiments after HA addition could be due to (1) electron shuttling via dissolved HA (Lovley et al., 1996b; Royer et al., 2002a; Jiang and Kappler, 2008), (2) Fe(III) solubilization by complexation (Lovley et al., 1996a; Nevin and Lovley, 2002a), (3) scavenging of dissolved Fe(II) thereby maintaining the thermodynamic driving force for further Fe(III) reduction (Royer et al., 2002b) and decreasing Fe(II) sorption, or (4) potentially even facilitating electron transfer through sorbed HA (Marsili et al., 2008). In order to evaluate the actual mechanism responsible for the acceleration, we quantified the adsorbed and dissolved fractions of HA present in our experiments.

After adding HA at total concentrations from 50 to 400 mg/l to the Fe(III)-reducing cultures, quantification of HA in the culture supernatant showed that a significant

Table 1
Concentration of total and dissolved Pahokee Peat Humic Acid (HA) and calculated concentration of Fe(II) complexed by dissolved HA in cultures containing 5 or 30 mM of ferrihydrite. HA concentrations were determined by UV analysis. For calculation of Fe(II) complexation see Appendix 6 in Supplementary data.

HA total (mg/l)	5 mM Ferrihydrite		30 mM Ferrihydrite	
	HA dissolved (mg/l)	Complexed Fe(II) (mM)	HA dissolved (mg/l)	Complexed Fe(II) (mM)
48.9	14.4	0.11	n.d.	0.00
94.8	47.6	0.35	n.d.	0.00
191.7	126.6	0.93	n.d.	0.00
390.4	318.0	2.33	7.4	0.05

n.d.: not detectable = below detection limit of instrument (0.01 mg/l).

fraction of the added HA was adsorbed to the mineral surface (Table 1). In the 5 mM ferrihydrite setups, dissolved HA concentrations between 14.4 and 318.0 mg/l were measured, indicating that in all 5 mM ferrihydrite setups dissolved HA was present (Table 1). Doubling of the total HA concentration from 191.7 mg/l to 390.4 mg/l lead to an almost equivalent increase of 191.4 mg/l in dissolved HA concentrations (from 126.6 to 318.0 mg/l, Table 1), meaning that virtually no additional HA were sorbed to the mineral surface due to surface saturation with HA. This was confirmed by HA sorption isotherms (based on the Langmuir equation) for 5 mM ferrihydrite (Appendix 4 in Supplementary data). Calculations based on the isotherm data yielded maximum amounts of 145 mg HA sorbed per g ferrihydrite in phosphate containing solutions and 292 mg HA per g ferrihydrite in the absence of phosphate at total concentrations of approximately 310 mg HA/l and 530 mg HA/l, respectively (Appendix 4 in Supplementary data). The differences in sorption maxima with and without phosphate showed that competitive sorption of phosphate and HA occurred at the mineral surface. In presence of 30 mM ferrihydrite, surface saturation was not achieved at any HA concentration used in our experiments. Consequently, in all 30 mM ferrihydrite setups there was an excess of mineral surface sites relative to sorbed HA molecules present. The mineral surface was therefore just partially covered with HA molecules. The highest HA concentration of 400 mg/l resulted in a dissolved HA concentration of 7.4 mg/l (Table 1). This sorption behavior could also be observed visually. The liquid phase in the culture tubes containing 30 mM ferrihydrite remained clear after ferrihydrite sedimentation (with exception of the 400 mg/l setup), whereas in the 5 mM ferrihydrite setups a brownish-colored supernatant was observed at all HA concentrations (Fig. 1e and f).

A stimulation of microbial reduction by dissolved HA was observed in the 5 mM ferrihydrite setups where addition of HA increased Fe(III) reduction rates. The rates in presence of HA are not only higher than in phosphate-amended setups but also higher than in phosphate-free setups (Fig. 1c). The acceleration of Fe(III) reduction can be explained by the presence of significant concentrations of dissolved HA shuttling electrons from the cells to the Fe(III) minerals. In all 5 mM ferrihydrite setups the HA concentrations were above the lower limit of HA necessary for stimulation of Fe(III) reduction (10 mg/l dissolved HA) (Jiang and Kappler, 2008). From our data it can also be seen that after exceeding surface saturation of the mineral particles with adsorbed HA no further acceleration of iron reduction rates occurred. In presence of 5 mM ferrihydrite this was the case above a surface loading of 145 mg adsorbed HA/g ferrihydrite and 240 mg/l dissolved HA (Appendix 4 in Supplementary data). With further addition of HA the iron reduction rates remained at a constant elevated level, while the concentration of dissolved HA was still increasing (Table 1 and Fig. 1). Jiang and Kappler (2008) also suggested an upper limit of dissolved HA for electron shuttling (50 mg/l HA in experiments using 1 mM ferrihydrite in the presence of phosphate). This suggests that above a certain threshold concentration of dissolved HA – that may vary in individual experiments depending on surface area of minerals used, cell density, etc. – the electron transfer process may be limited either by the metabolic activity of the cells (i.e. by the oxidation rate of organic carbon and the release of a certain number of electrons per time) or by the electron transfer from dissolved (reduced) HA to the mineral surface that is limited by the number of surface sites available at the mineral surface.

In contrast to the 5 mM setups, in all 30 mM ferrihydrite setups the addition of HA did not stimulate Fe(III) reduction compared to the setups that contained neither HA nor phosphate. Only the addition of 50 mg/l HA led to an increase of the reduction rates compared to phosphate-containing setups. The inhibiting effect of phosphate was most likely compensated by the added HA via competitive sorption at surface sites (comparable to the sorption isotherms, Appendix 4 in Supplementary data). The low reduction rates observed even at higher HA concentrations suggest that despite the presence of a significant amount of HA, these sorbed HA molecules did not stimulate microbial Fe(III) reduction (for detailed discussion of the decrease in reduction rates with increasing HA concentration in the 30 mM experiments see section 3.4). Even in 30 mM ferrihydrite setups with addition of 400 mg/l HA where 7.4 mg/l of HA remained in solution, this amount was not sufficient to significantly stimulate microbial iron reduction (Fig. 1d). This observation is again in agreement with the study from Jiang and Kappler (2008), who showed that a minimum concentration of 10 mg/l dissolved HA is necessary to stimulate microbial ferrihydrite reduction.

Since all experiments with HA also contained phosphate, for comparison we performed experiments with 5 and 30 mM ferrihydrite and varying HA concentrations in the absence of

phosphate (Appendix 5 in Supplementary data). Similar to the phosphate-containing experiments, in the 30 mM ferrihydrite setups we observed complete sorption of HA (Appendix 5 Table A2 in Supplementary data) and no stimulation, rather inhibition, of microbial iron reduction (Fig. A5 in Supplementary data) at any of the HA concentrations tested (with even slightly lower rates than measured in the presence of phosphate). This supports the observation that sorbed HA molecules alone do not accelerate the electron transfer between bacteria and iron minerals, but rather negatively influence the mineral surface similar to sorbed phosphate. Experiments with 5 mM ferrihydrite conducted in the absence of phosphate showed complete HA sorption at the two lowest total HA concentrations (52.0 and 84.2 mg/l HA) (Table A2 in Supplementary data) causing a decrease in Fe(III) reduction rate (Fig. A5 in Supplementary data). At higher total HA concentrations (216.1, 320.2 and 518.4 mg/l HA) a significant fraction of HA was in solution (Table A2 in Supplementary data) and the Fe reduction rates increased with increasing concentrations of dissolved HA similar to the experiments in the presence of phosphate (Fig. A5 in Supplementary data). Therefore the general conclusions drawn from the phosphate-containing experiments regarding the effect of sorbed and dissolved HA on inhibition and stimulation of Fe(III) reduction remain the same also in absence of phosphate.

3.3. Importance of Fe(II) and Fe(III) complexation by HA for microbial ferrihydrite reduction

Besides facilitating electron transfer from cells to poorly soluble Fe(III) minerals by electron shuttling, dissolved HS also have been suggested to stimulate microbial Fe(III) reduction by Fe(II) complexation and thus removal of the metabolic product, i.e. Fe(II), thereby maintaining the thermodynamic driving force for further reduction (Royer et al., 2002a,b). Consequently, with increasing concentrations of dissolved HA more Fe(II) is expected to be complexed, thus more Fe(III) is expected to be reduced at a likely higher reduction rate. To determine whether this mechanism played a role in our experiments, we calculated the theoretical amount of Fe(II) that can be complexed by the dissolved HA present, based on the content of acidic functional groups given by the IHSS (Table 1, Appendix 6 in Supplementary data). According to these calculations, 126.6 and 318.0 mg/l dissolved HA should complex 0.93 and 2.33 mM Fe(II), respectively (Table 1, Appendix 6 in Supplementary data). Consequently an increase of the total HA concentration from 200 to 400 mg/l in presence of 5 mM ferrihydrite should have a major effect on the Fe(II) complexation and thus on the iron reduction rates. However, the reduction rates were almost the same in the 200 and 400 mg/l setups and no further increase in total Fe(II) formed was observed. We therefore conclude that Fe(II) complexation played a minor role for stimulation of Fe(III) reduction in our experiments. In addition to complexation of Fe(II), HA can also complex and solubilize Fe(III). We observed low Fe(III) concentrations (0.1 mM) in HA filtrates after incubating HA with ferrihydrite in the absence of Fe(III)-reducing cells for three weeks (data not shown). Although we did not quantify the kinetics of this complexation reaction in detail, this process did probably also occur to a low extent during incubation of the ferrihydrite/HA mixtures with Fe(III)-reducing cells (however, the dissolved Fe(III) concentration remained below the detection limit during the experiments). Therefore, we cannot exclude the influence of low amounts of complexed Fe(III), as suggested by Nevin and Lovley (2002a), on the observed increase in iron reduction rates with increasing HA concentrations.

3.4. Effect of HA-iron mineral aggregation on the accessibility of iron minerals

Our experiments showed that, depending on the concentrations of ferrihydrite and HA, HA either stimulated microbial Fe(III) reduction by electron shuttling or inhibited Fe(III) reduction. The absence of a clear correlation between Fe(III) reduction rates and HA concentration observed in the 30 mM ferrihydrite setups showed that another effect, besides surface blocking due to HA sorption, obviously played a role. Visual observation of the glass culture tubes showed differences in particle sedimentation behaviour at different ferrihydrite and HA concentrations (Fig. 2), leading to the hypothesis that the ferrihydrite aggregate size and thus the surface area available for bacterial electron transfer were different at the two different ferrihydrite concentrations. This is important since microbial Fe(III) reduction can depend on the available surface area of the Fe(III) mineral (Roden and Zachara, 1996; Roden, 2003).

The size of the ferrihydrite aggregates differed even in the absence of HA at the two ferrihydrite concentrations used, with larger aggregates and faster sedimentation in the 30 mM compared to the 5 mM setup (Figs. 2a and 3a and b, Appendix 7 in Supplementary data). Microscopy images suggested small but visible differences between the 5 mM and the 30 mM setups (Fig. 3a and b) and in particular the observed sedimentation speed and visual observation of the aggregates (Fig. 2a) clearly indicate a different size distribution of the ferrihydrite aggregates between the two concentrations investigated. However, not only ferrihydrite concentration but also the presence of HA influenced the aggregate formation. In all 5 mM ferrihydrite setups the HA-coated ferrihydrite particles were distributed almost homogeneously in the culture tube even after a few minutes and settled very slowly (Fig. 2b). Confocal laser scanning microscopy images showed mostly small, individual mineral particles for 5 mM setups, sometimes also a few larger particles, in particular in HA-containing setups (Fig. 3a, c and e, Appendix 7 in Supplementary data). In contrast, 30 mM ferrihydrite setups amended with 0–200 mg HA/l showed aggregated mineral particles (Fig. 3b, d and f, Appendix 7 in Supplementary data) and faster sedimentation than in the 5 mM ferrihydrite containing setups (Fig. 2c). Only after addition of 400 mg/l HA to 30 mM ferrihydrite the sedimentation was slow with a speed comparable to the speed observed for the 5 mM ferrihydrite setups. Comparing these results from sedimentation experiments to the concentrations of dissolved HA (Table 1) showed that in all setups containing dissolved HA the sedimentation was slow, suggesting the presence of small-sized particles, while in the absence of detectable amounts of dissolved HA, sedimentation was rapid

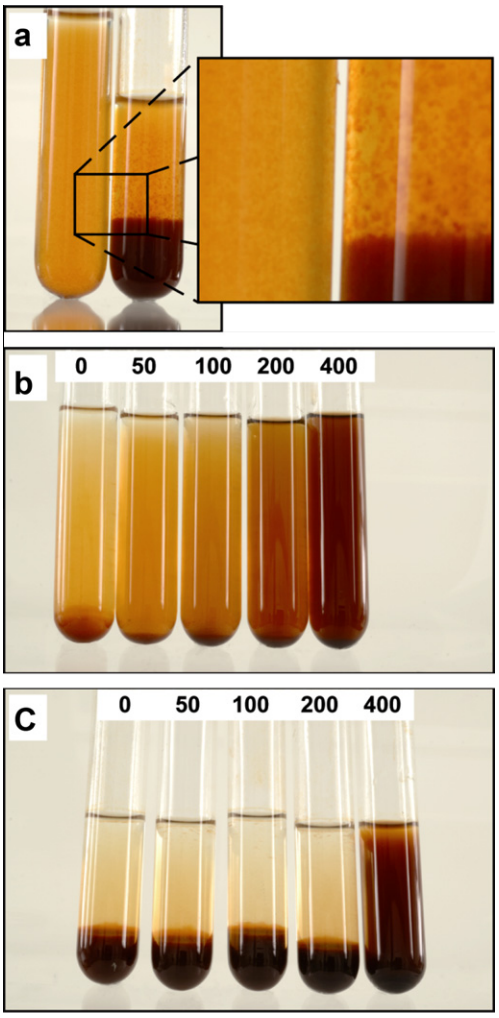

Fig. 2. Ferrihydrite particle aggregation indicated by sedimentation behaviour of mineral particles before bacterial inoculation. Image (a) shows tubes that contain 5 mM (left tube) and 30 mM ferrihydrite (right tube) without any additions. Images were taken 2 min after shaking. Note the difference in ferrihydrite aggregate size visible in the close-up image. Image (b) shows tubes containing 5 mM and image (c) 30 mM ferrihydrite with and without addition of HA. Images were taken 10 min after shaking. Pictures show, from left to right, tubes containing 0, 50, 100, 200 and 400 mg/l HA (total concentrations; all tubes contain 0.8 mM phosphate buffer).

due to larger mineral aggregates. Interestingly, the 30 mM ferrihydrite setup containing 400 mg/l HA showed slow sedimentation similar to 5 mM containing setups (Fig. 2) but also large aggregates in the microscopy images (Fig. 3f). The associated HA may have lowered the density of the large aggregates enough so they could stay in the water column for a longer time than aggregates formed in presence of lower HA concentrations. In any case, the 400 mg/l HA setup contained large aggregates that showed a lower bioaccessibility and therefore lower reduction rates (see discussion below) (Fig. 1).

Since our results suggest that the presence of sorbed HA influenced ferrihydrite aggregation and microbial electron transfer to ferrihydrite, it is necessary to understand the geochemical factors controlling the aggregation of such particles. Vermeer et al. (1998) showed that adsorption of negatively charged HA molecules to positively charged iron minerals lowered the point of zero charge (pzc) of hematite. They also found less HA sorption on small hematite particles compared to large ones due to higher negative surface charge density of small HA-coated hematite particles. Strong repulsion between the negatively charged, small, HA-coated hematite particles and additional negatively charged dissolved HA molecules prevented further HA adsorption. In addition, it has been shown that the change in surface charge by adsorption of HA to colloidal magnetite particles increased the stability of colloidal magnetite dispersions, probably due to repulsion of the negatively charged particles, preventing aggregation (Illés and Tombácz, 2006).

A similar stabilization of small mineral particles probably occurred in our 5 mM ferrihydrite experiments, where the mineral particles were relatively small in the absence of HA (Figs. 2a and 3a and c). Adsorption of HA to these small ferrihydrite aggregates led to a high negative charge density on the aggregates, which caused a stabilization or further disintegration of the present iron mineral aggregates (Fig. 3c and e). Particle aggregation was obviously prevented and led to a high surface area per amount of ferrihydrite with less intra-aggregate sites and good access for microbial cells to surface sites for electron transfer. The simultaneous presence of dissolved HA which we observed in our experiments with 5 mM ferrihydrite additionally promoted iron reduction by the dissolved HA acting as electron shuttle (Fig. 1c).

In presence of 30 mM ferrihydrite and HA concentrations >50 mg/l, reduction rates decreased to values even lower than in the absence or presence of just phosphate (Fig. 1d), indicating that the ferrihydrite surface available for the Fe(III)-reducing bacteria further decreased. This could be due to further aggregation instead of electrostatic repulsion of charged particles (in contrast to the 5 mM ferrihydrite setups) after inhomogeneous sorption of negatively charged HA to the positively charged, larger primary particles. Confocal laser scanning microscopy images support this conclusion showing larger mineral aggregates for the higher ferrihydrite concentration, especially in presence of HA (Fig. 3f, Appendix 7 in Supplementary data). Illés and Tombácz (2006) described the non-uniform distribution of negatively charged HS on the positively charged magnetite surface as “patch-wise charge heterogeneity”, leading to electrostatic attraction between the patches of opposite charge on the mineral surface and promoting aggregation of the particles. In this case, HA act as bridging molecules between mineral particles. The particle aggregation leading to more intra-aggregate sites and a decrease in available surface sites for Fe(III) reduction (Fig. 3f), in combination with the lack of dissolved HA, probably explains the observed low reduction rates in presence of 100–400 mg/l HA (Fig. 1d). The fact that the reduction rate was slightly higher in presence of 50 mg/l HA suggests that at this HA concentration the amount of HA sorbed to mineral aggregates was probably not high enough to cause significant particle aggregation.

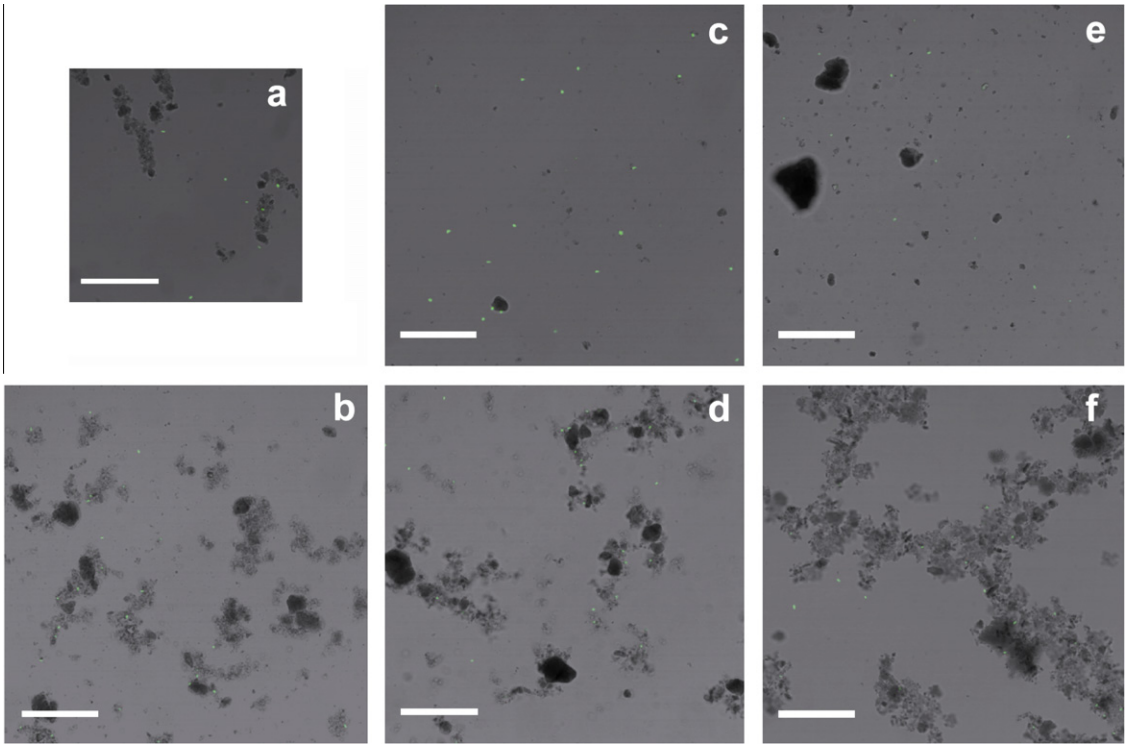

Fig. 3. Overlay of fluorescence and light microscopy images showing the localization of bacterial cells (green spots) and ferrihydrite particles (dark areas) directly after inoculation and before incubation. The different panels show cultures containing 5 mM (upper row) and 30 mM ferrihydrite (bottom row). Setups contain medium, ferrihydrite, cells and (a and b) no additions, (c and d) 0.8 mM phosphate, or (e and f) 0.8 mM phosphate + 400 mg/l HA. All scale bars equal 50 μm. More images are shown in Appendix 7 in Supplementary data.

3.5. Consequences of HA-mineral aggregate formation for electron shuttling and Fe(III) reduction rates

As demonstrated, HA can either stimulate Fe(III) reduction by electron shuttling or hinder electron transfer by sorption, surface blocking and/or aggregate formation leading to a decreased amount of bioaccessible surface sites. The scheme in Fig. 4 illustrates and summarizes the complex interplay of the main components in our experimental system of iron minerals, HA, phosphate and Fe(III)-reducing bacteria, considering the effects of phosphate and varying concentrations of HA and ferrihydrite.

The changes in ferrihydrite sedimentation behavior showed that at the higher ferrihydrite concentration the ferrihydrite aggregates are larger, and thus the accessible surface area per mass ferrihydrite decreases (see illustration in Fig. 4a and b). Sorption of phosphate to the mineral surface blocks surface sites for electron transfer leading to decreased reduction rates (Figs. 1c and d 4c and d). The additional presence of HA seems to partially outweigh the inhibiting effect caused by phosphate, potentially due to competitive sorption on ferrihydrite particles (Fig. 4e and f). However, the presence of HA did not show an acceleration of microbial Fe(III) reduction under each condition investigated (Fig. 1c and d). In fact, HA sorption can block surface sites on the mineral and restrict the accessibility for bacteria. Furthermore, the negatively charged cells compete with the negatively charged HA (and phosphate) for sorption sites also lowering the number of cells present at the mineral surface as evidenced by the confocal laser scanning microscopy images (Fig. 3, Appendix 7 in Supplementary data). Additionally, and probably even more important, negatively charged HA molecules (and phosphate) bind to ferrihydrite particles, change the net surface charge of the iron mineral particles from positive to negative (at least partially) and depending on the size of the ferrihydrite particles, lead either to repulsion of the particles and disintegration of small aggregates (Figs. 4c, e, g and 3c and e) or to formation of larger iron mineral-HA aggregates (Figs. 4f, h and 3f). These larger ferrihydrite-HA aggregates are less accessible for bacteria either due to their smaller surface area per mass ferrihydrite (in comparison to the non-aggregated ferrihydrite particles) or due to repulsion of negatively charged cells by the negatively charged mineral surface (Fig. 4f and h). Both effects lead to lower reduction rates. The aggregation effect resulting in a lowered bioaccessible surface area can be observed at low HA to ferrihydrite ratios (30 mM ferrihydrite experiments, Fig. 1d). In this case either none or only very few HA molecules are present in solution not supporting electron shuttling and requiring direct contact between cells and the mineral surface for electron transfer. In the presence of low ferrihydrite concentrations (5 mM), a further increase of the HA:ferrihydrite ratio leads to the presence of significant concentrations of dissolved HA (Table 1). Once the minimum amount of 10 mg/l dissolved HA necessary for

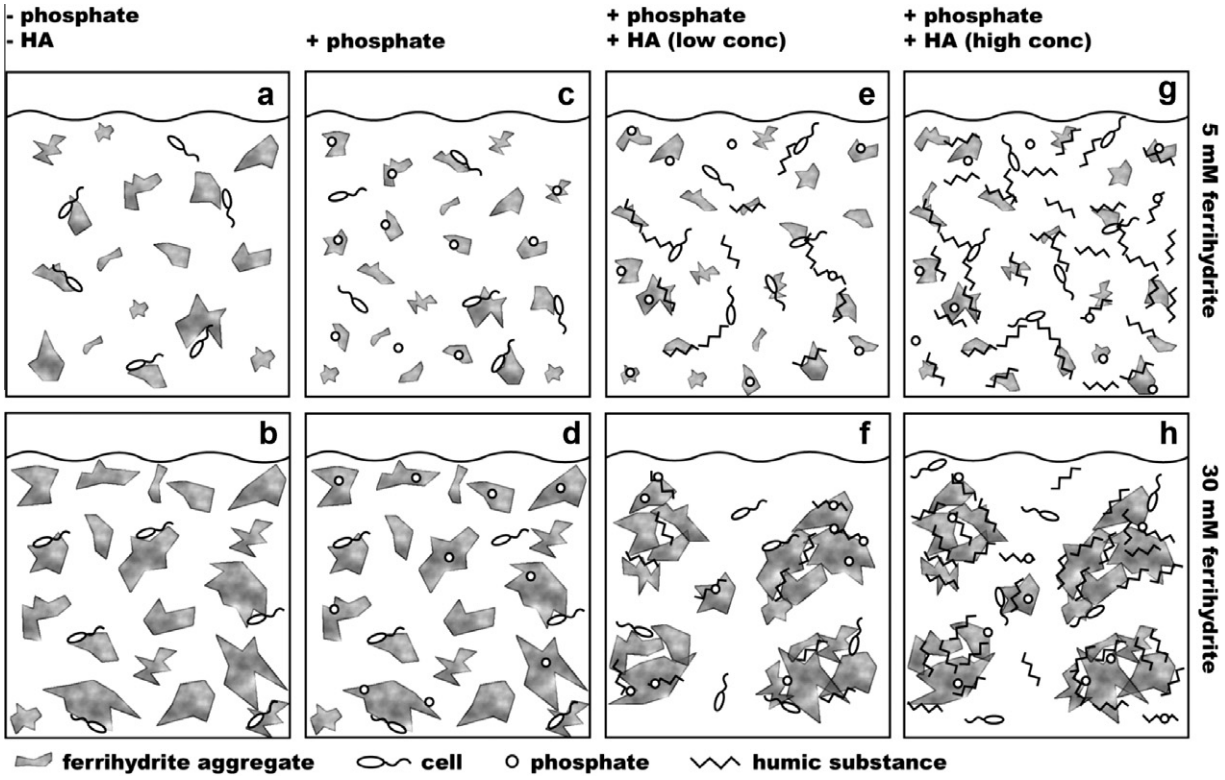

Fig. 4. Schematic illustration of changes in size of mineral aggregates, aggregate surface area and coverage of the aggregates by cells, phosphate and HA. The different panels illustrate cultures containing 5 mM (upper row) and 30 mM ferrihydrite (bottom row). All setups contain medium, ferrihydrite and cells. The concentrations of phosphate and humic acids (HA) vary in the different diagrams as indicated above the diagrams.

electron shuttling is reached, microbial reduction is stimulated (Figs. 1c and 4e). Dissolved HA effectively shuttle electrons between cells and ferrihydrite superseding the need for direct contact between cells and the mineral surface. However, the stimulating effect (indicated by increasing reduction rates) levels off as soon as the mineral surface is saturated with adsorbed HA in presence of more than 200 mg/l total HA (Figs. 1c and 4g). This suggests an upper limit of dissolved HA concentration above which the reduction rate is no longer limited by the electron transfer between cells and ferrihydrite via dissolved HA but rather by the release of electrons from the cells or the electron transfer from dissolved HA to the limited number of surface sites on the mineral surface. In summary, we conclude that the rates of electron transfer from Fe(III)-reducing cells to ferrihydrite (including HA electron shuttling) strongly depend on the HA:ferrihydrite ratio, on aggregate sizes, on the sorption capacity of ferrihydrite for HA, and thus on the proportions of dissolved and adsorbed HA.

3.6. Effect of phosphate and HA on mineral (trans)formation during microbial Fe(III) reduction

The presence of both phosphate and HA are expected to influence mineral formation during microbial Fe(III) reduction. We therefore identified the minerals produced by μ-XRD and for some experiments also by ^{57}Fe-specific Mössbauer spectroscopy (Figs. 5 and 6). Additionally, we quantified dissolved, loosely bound, poorly crystalline and crystalline Fe species by sequential extraction (Fig. 7).

The influence of phosphate on the identity of the minerals formed was most obvious for experiments containing 5 mM ferrihydrite. During the fast and almost complete microbial reduction, biogenic Fe(II) precipitates were formed in presence of phosphate (Fig. 5a) while in the absence of phosphate only dissolved Fe^{2+} remained (extraction data not shown). The Fe(II) minerals that formed were identified as vivianite by Mössbauer spectroscopy (Fig. 5a) and XRD (Fig. A6, Appendix 8 in Supplementary data) both in absence and presence of HA. In these experiments the ferrihydrite surface available for Fe(II) adsorption was depleted too fast to promote solid phase conversion of ferrihydrite to magnetite or recrystallization to goethite or lepidocrocite. Instead, the formed Fe(II) remained in solution as Fe^{2+} or, in the presence of phosphate, precipitated as vivianite, as similarly reported in previous studies (Kukkadapu et al., 2004; Borch et al., 2007). In contrast to the 5 mM ferrihydrite setups, cultures containing 30 mM ferrihydrite showed formation of magnetite and goethite during reduction by *Shewanella oneidensis MR-1* (Figs. 5b and 6). These observations agree well with earlier findings of goethite and magnetite formation during microbial ferrihydrite reduction (Hansel et al., 2003; Borch et al., 2007;Piepenbrock et al., 2011).

While the influence of phosphate on biogenic (trans)formation of iron minerals has been the subject of several studies

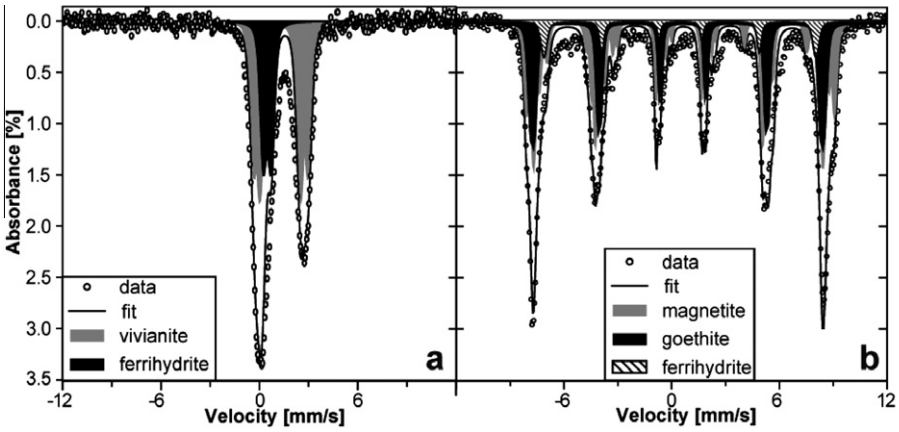

Fig. 5. Mössbauer spectra of ferrihydrite reduced by *Shewanella oneidensis* MR-1. (a) 5 mM Ferrihydrite reduced in presence of 0.8 mM phosphate, after 11 days of incubation (measured at 77 K). (b) 30 mM of ferrihydrite reduced, after 9 days of incubation (measured at 4.2 K). Open circles: measured data, filled areas: modelled relative amounts of identified minerals, solid line: fitted spectrum.

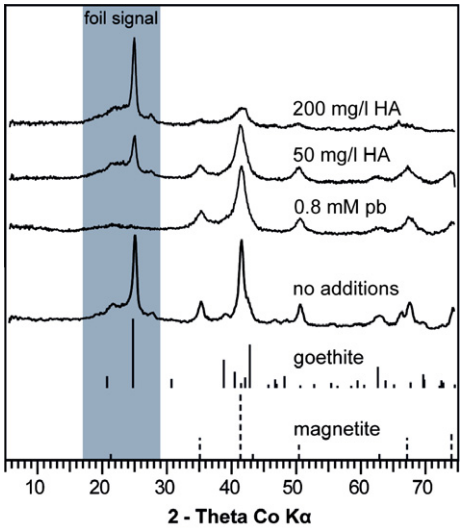

Fig. 6. X-ray diffractograms of precipitates formed during reduction of 30 mM ferrihydrite by *Shewanella oneidensis* MR-1 in presence of 50 and 200 mg/l HA, respectively. Furthermore, reference experiments without additions and in the presence of 0.8 mM phosphate buffer (pb) are shown. Samples were collected after Fe(III) reduction stopped. Reference patterns of magnetite and goethite are shown for comparison. The gray bar indicates the signal of the foil covering the sample holder to maintain anoxic conditions during measurements. The sample with phosphate buffer was measured without the protecting polyethylene foil.

(Fredrickson et al., 1998; Borch et al., 2007), the effect of HA on mineral identity during ferrihydrite reduction has not been studied in detail and will be discussed here in particular for our experiments with 30 mM ferrihydrite. However, the general effects of HA on Fe mineralogy discussed here for the 30 mM ferrihydrite data hold also true for the experiments with HA and 5 mM ferrihydrite (see Appendix 8 in Supplementary data). For all setups containing 30 mM ferrihydrite we identified magnetite as mineral product, goethite was only present in the absence of phosphate or HA (Fig. 6). A quantitative analysis of this Mössbauer spectrum (Fig. 5b) showed the formation of 69% magnetite, 24% goethite and a residual amount of 7% ferrihydrite at the end of microbial reduction. This ratio suggests topotactic conversion to magnetite over Fe(II)-induced recrystallization to goethite as preferential conversion mechanism. Additionally, XRD analysis of precipitates formed in presence of HA and phosphate showed lower intensities and broader signals than samples taken from HA- and phosphate-free cultures (Fig. 6). The broadening of the reflections became even more pronounced with increasing HA concentrations. This indicates the formation of iron minerals that show more short range ordering and/or smaller particle size due to sorption of phosphate and/or HA to the mineral surface during mineral formation.

Studies investigating the effect of phosphate on mineral reduction (Hansel et al., 2003; Borch et al., 2007) showed formation of different minerals during ferrihydrite reduction by *Shewanella putrefaciens* strain CN32 in the presence or absence of phosphate. They observed that higher crystalline phases like goethite were exclusively formed in absence of phosphate. Abiotic experiments showed that phosphate hinders the transformation of ferrihydrite to goethite or hematite (Gálvez et al., 1999). Blocking of the ferrihydrite surface prevents Fe(II) sorption, thus decreasing the density of sites occupied with Fe(II) and lowering the number of surface sites where conversion of ferrihydrite to magnetite or goethite can take place. Additionally, magnetite crystallization (crystal growth) can be inhibited by the presence of phosphate by blocking specific crystal faces (Couling and Mann, 1985). Another abiotic study on precipitation of ferrihydrite described a significant decrease in particle size and structural order of ferrihydrite with increasing organic matter to iron ratios (Eusterhues et al., 2008). This means sorption of phosphate and HA to newly forming crystallites prevents the formation of large crystal domains and therefore limits the formation of more crystalline minerals such as goethite.

In order to quantify the distribution of Fe(II) and Fe(III) in the dissolved, loosely bound, poorly crystalline and crystalline fractions at different stages of ferrihydrite reduction, we used a sequential extraction procedure (Fig. 7). Generally (independent of whether phosphate

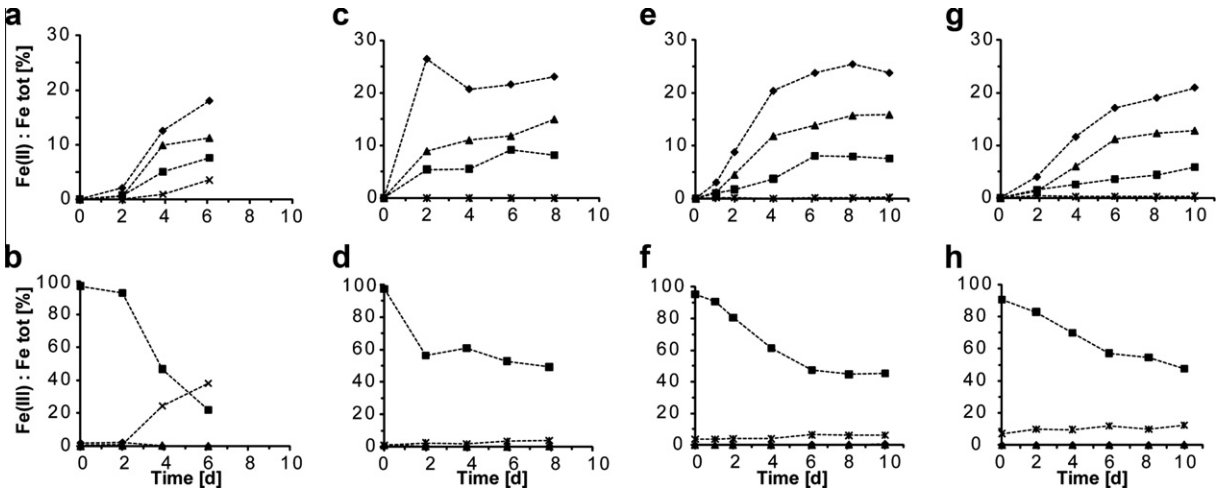

Fig. 7. Dissolved (▲), loosely bound (♦), poorly crystalline (■) and crystalline (×) Fe(II) fractions (top row) and Fe(III) fractions (bottom row) quantified by sequential extraction of precipitates formed during microbial reduction of 30 mM ferrihydrite (a and b) no additions, (c and d) with 0.8 mM phosphate (e and f) with 50 mg/l HA + 0.8 mM phosphate and (g and h) with 200 mg/l HA + 0.8 mM phosphate. Figures show representative data from independent experiments. Please note the different scales (y-axis) in the upper and lower row. Data points are connected as a guide to the eye. A Table of measured data from this diagram is given in Appendix 9 in Supplementary data.

and/or HA were present), the highest Fe(II) concentrations were detected in the fraction of loosely bound Fe(II), some Fe(II) stayed in solution, some was bound in the poorly crystalline fraction and the lowest amount of Fe(II) was present in the crystalline fraction. Also, in all setups we did not detect significant amounts of Fe(III) in the fraction of dissolved iron. However, we observed distinct differences in the crystalline fraction depending on the presence of phosphate or HA. The presence of magnetite and goethite identified by Mössbauer spectroscopy and XRD in HA- and phosphate-free setups (Figs. 5b and 6) was confirmed by the presence of Fe(II) and Fe(III) in the crystalline fraction (Fig. 7a and b). In contrast, after addition of phosphate and with increasing concentrations of HA no Fe(II) was found in the crystalline fraction and the Fe(III) fraction shifted towards poorly crystalline species (Fig. 7). In summary, the sequential extraction data reveal the following trends: (1) Fe(II) (and to a great extent Fe(III)) bound in crystalline phases was only detectable in the absence of phosphate or HA (Fig. 7a and b), (2) addition of phosphate or HA led to an increase of Fe(II) present in dissolved or adsorbed form (Fig. 7c, e and g) and (3) the majority of Fe(III) was present in poorly crystalline form (Fig. 7d, f and h). Overall, this suggests together with the spectroscopic analysis of the minerals that the solubility of the biogenic magnetite increased in the presence of phosphate and HA due to the formation of smaller mineral particles and/or a decreased order in the crystal structure.

4. CONCLUSIONS

In this study we evaluated how the presence of HA influenced microbial reduction of the Fe(III) mineral ferrihydrite at neutral pH. We found that electron shuttling via HA cannot be enhanced infinitely by increasing amounts of HA but electron shuttling is rather restricted to a relatively narrow range of dissolved HA concentrations with increasing rates with increasing HA concentrations from ~10–240 mg/l HA. This suggests that electron shuttling is of minor importance in anoxic groundwater aquifers that contain HS concentrations mostly below the concentration range that can stimulate electron transfer from cells to Fe(III) minerals (e.g. 0.4 mg/l in groundwater, (Aiken, 1985)). We also found that depending on iron mineral and HS concentrations, HS do not only stimulate but also lower electron transfer rates to ferrihydrite by sorption to the ferrihydrite surface leading to particle aggregation and thus to a decreased bioavailable surface area. Obviously both dissolved and ferrihydrite-sorbed HA influence microbial electron transfer from cells to ferrihydrite. Therefore, seasonal changes of HS concentrations for example due to flooding events in rice paddy fields can have a large impact on iron mineral turnover rates and on biogeochemical iron cycling.

The observed changes in mineral crystallinity in the presence of humic compounds have to be considered when evaluating the reactivity of Fe minerals in the environment. It has been shown that crystalline Fe(III) minerals such as goethite, akaganeite, hematite and magnetite are reduced at much lower rates and only to a smaller extent compared to poorly crystalline ferrihydrite (Lovley and Phillips, 1988). Similar observations were made for the microbial oxidation of reduced iron minerals by iron-oxidizing bacteria. While more soluble minerals such as siderite were oxidized by anoxygenic phototrophic Fe(II)-oxidizing bacteria, more crystalline or less soluble minerals such as vivianite and magnetite were not oxidized by the same bacteria (Kappler and Newman, 2004). In addition, the crystallinity of the mineral products also controls the further reactivity of the minerals. Fe(II) sorbed to Fe(III) minerals with low crystallinity was less efficient in the reductive transformation of organic pollutants under anoxic conditions than Fe(II) sorbed to highly crystalline Fe(III) minerals such as hematite (Elsner et al., 2004). Therefore

biogenic minerals formed in presence of phosphate or HA, similar to our precipitates, do have a higher potential to be involved in biogeochemical cycling of Fe but very likely also show a lower efficiency in reductive transformation of contaminants.

In summary our results suggest that iron cycling in environmental systems not only depends on pH, solute chemistry, microbial strains, reduction mechanisms involved and the identity of initially present minerals, but also on the aggregation state of Fe minerals as controlled by HS (i.e. by the HS:Fe ratio) or by the concentration of the mineral itself. Therefore, the effect of HS-induced Fe mineral aggregation on microbial iron mineral transformation and reactivity has to be included in the framework of environmental iron biogeochemistry.

ACKNOWLEDGEMENTS

This work was funded by the German Research Foundation to A.K. and, in part, by a National Science Foundation (NSF) CAREER Award (EAR 0847683) to T.B. We would like to thank Dr. Kristina Straub for advice on microbiological work, Dr. Christoph Berthold for help with XRD measurements, Florian Hegler for confocal laser scanning microscopy images and Philip Larese-Casanova for Mössbauer measurements and their interpretation. Comments by Stefan Haderlein, Philip Larese-Casanova and three anonymous reviewers greatly improved the quality of the manuscript.

APPENDIX A. SUPPLEMENTARY DATA

Supplementary data associated with this article can be found, in the online version, at http://dx.doi.org/10.1016/j.gca.2012.02.003.

REFERENCES

Aiken G. R. (1985) *Humic substances in soil, sediment, and water: geochemistry, isolation, and characterization*. Wiley, New York.

Ardizzone S. and Formaro L. (1983) Temperature induced phase transformation of metastable $Fe(OH)_3$ in the presence of ferrous ions. *Mater. Chem. Phys.* **8**, 125–133.

Bauer I. and Kappler A. (2009) Rates and extend of reduction of Fe(III) compounds and O_2 by humic substances. *Environ. Sci. Technol.* **43**, 4902–4908.

Borch T., Masue Y., Kukkadapu R. K. and Fendorf S. (2007) Phosphate imposed limitations on biological reduction and alteration of ferrihydrite. *Environ. Sci. Technol.* **41**, 166–172.

Borch T., Kretzschmar R., Kappler A., Cappellen P. V., Ginder-Vogel M., Voegelin A. and Campbell K. (2010) Biogeochemical redox processes and their impact on contaminant dynamics. *Environ. Sci. Technol.* **44**, 15–23.

Coates J. D., Ellis D. J., Blunt-Harris E. L., Gaw C. V., Roden E. E. and Lovley D. R. (1998) Recovery of humic-reducing bacteria from a diversity of environments. *Appl. Environ. Microbiol.* **64**, 1504–1509.

Coker V. S., Bell A. M. T., Pearce C. I., Pattrick R. A. D., van der Laan G. and Lloyd J. R. (2008) Time-resolved synchrotron powder X-ray diffraction study of magnetite formation by the Fe(III)-reducing bacterium Geobacter sulfurreducens. *Am. Miner.* **93**, 540–547.

Cornell R. M. and Schwertmann U. (2003) *The Iron Oxides*. Wiley-VCH Verlag GmbH & Co, KGaA, Weinheim.

Couling S. B. and Mann S. (1985) The influence of inorganic phosphate on the crystallization of magnetite (Fe_3O_4) from aqueous solution. *J. Chem. Soc., Chem. Commun*, 1713–1715.

Ekstrom E. B., Learman D. R., Madden A. S. and Hansel C. M. (2010) Contrasting effects of Al substitution on microbial reduction of Fe(III) (hydr)oxides. *Geochim. Cosmochim. Acta* **74**, 7086–7099.

Elsner M., Schwarzenbach R. P. and Haderlein S. B. (2004) Reactivity of Fe(II)-bearing minerals toward reductive transformation of organic contaminants. *Environ. Sci. Technol.* **38**, 799–807.

Eusterhues K., Wagner F. E., Häusler W., Hanzlik M., Knicker H., Totsche K. U., Kögel-Knabner I. and Schwertmann U. (2008) Characterization offerrihydrite-soil organic matter Coprecipitates by X-ray diffraction and Mössbauer spectroscopy. *Environ. Sci. Technol.* **42**, 7891–7897.

Fredrickson J. K., Kota S., Kukkadapu R. K., Liu C. and Zachara J. M. (2003) Influence of electron donor/acceptor concentrations on hydrous ferric oxide (HFO) Bioreduction. *Biodegradation* **14**, 91–103.

Fredrickson J. K., Zachara J. M., Kennedy D. W., Dong H., Onstott T. C., Hinman N. W. and Li S.-m. (1998) Biogenic iron mineralization accompanying the dissimilatory reduction of hydrous ferric oxide by a groundwater bacterium. *Geochim. Cosmochim. Acta* **62**, 3239–3257.

Gálvez N., Barrón V. and Torrent J. (1999) Effect of phosphate on the crystallization of hematite, goethite, and epidocrocite from ferrihydrite. *Clays Clay Miner.* **47**, 304–311.

Gorby Y. A., Yanina S., McLean J. S., Rosso K. M., Moyles D., Dohnalkova A., Beveridge T. J., Chang I. S., Kim B. H., Kim K. S., Culley D. E., Reed S. B., Romine M. F., Saffarini D. A., Hill E. A., Shi L., Elias D. A., Kennedy D. W., Pinchuk G., Watanabe K., Ishii S. i., Logan B., Nealson K. H. and Fredrickson J. K. (2006) Electrically conductive bacterial nanowires produced by Shewanella oneidensis strain MR-1 and other microorganisms. *Proc. Natl. Acad. Sci. USA* **103**, 11358–11363.

Hansel C. M., Benner S. G., Neiss J., Dohnalkova A., Kukkadapu R. K. and Fendorf S. (2003) Secondary mineralization pathways induced by dissimilatory iron reduction of ferrihydrite under advective flow. *Geochim. Cosmochim. Acta* **67**, 2977–2992.

Illés E. and Tombácz E. (2006) The effect of humic acid adsorption on pH-dependent surface charging and aggregation of magnetite nanoparticles. *J. Colloid Interface Sci.* **295**, 115–123.

Jiang J. and Kappler A. (2008) Kinetics of microbial and chemical reduction of humic substances: implications for electron shuttling. *Environ. Sci. Technol.* **42**, 3563–3569.

Kaiser K., Mikutta R. and Guggenberger G. (2007) Increased stability of organic matter sorbed to ferrihydrite and goethite on aging. *Soil Sci. Soc. Am. J.* **71**, 711–719.

Kappler A. and Newman D. K. (2004) Formation of Fe(III)-minerals by Fe(II)-oxidizing photoautotrophic bacteria. *Geochim. Cosmochim. Acta* **68**, 1217–1226.

Kappler A. and Straub K. L. (2005) Geomicrobiological cycling of iron. In *Molecular Geomicrobiology* (eds. J. F. Banfield, J. Cervini-Silva and K. M. Nealson). The Mineralogical Society of America, Chantilly, Virginia, USA.

Konhauser K. O., Lalonde S. V. and Phoenix V. R. (2008) Bacterial biomineralization: Where to from here? *Geobiology* **6**, 298–302.

Konhauser K. O., Kappler A. and Roden E. E. (2011) Iron in microbial metabolisms. *Elements* **7**, 89–93.

Kretzschmar R. and Sticher H. (1997) Transport of humic-coated iron oxide colloids in a sandy soil: influence of Ca^{2+} and trace metals. *Environ. Sci. Technol.* **31**, 3497–3504.

Kukkadapu R. K., Zachara J. M., Fredrickson J. K. and Kennedy D. W. (2004) Biotransformation of two-line silica-ferrihydrite by a dissimilatory Fe(III)-reducing bacterium: formation of carbonate green rust in the presence of phosphate. *Geochim. Cosmochim. Acta* **68**, 2799–2814.

Lies D. P., Hernandez M. E., Kappler A., Mielke R. E., Gralnick J. A. and Newman D. K. (2005) Shewanella oneidensis MR-1 uses overlapping pathways for iron reduction at a distance and by direct contact under conditions relevant for biofilms. *Appl. Environ. Microbiol.* **71**, 4414–4426.

Lovley D. R. (2008) Extracellular electron transfer: wires, capacitors, iron lungs, and more. *Geobiology* **6**, 225–231.

Lovley D. R. and Phillips E. J. P. (1988) Novel mode of microbial energy metabolism: organic Carbon oxidation coupled to dissimilatory reduction of iron or manganese. *Appl. Environ. Microbiol.* **54**, 1472–1480.

Lovley D. R., Woodward J. C. and Chapelle F. H. (1996a) Rapid anaerobic benzene oxidation with a variety of chelated Fe(III) forms. *Appl. Environ. Microbiol.* **62**, 288–291.

Lovley D. R., Coates J. D., Blunt-Harris E. L., Phillips E. J. P. and Woodward J. C. (1996b) Humic substances as electron acceptors for microbial respiration. *Nature* **382**, 445–448.

Lovley D. R., Holmes D. E. and Nevin K. P. (2004) *Dissimilatory Fe(III) and Mn(IV) eeduction*. Academic Press, Adv. Microb. Physiol.

Mann S. (2001) *Biomineralization: Principles and Concepts in Bioinorganic Materials Chemistry*. Oxford University Press, Inc., New York, Oxford.

Marsili E., Baron D. B., Shikhare I. D., Coursolle D., Gralnick J. A. and Bond D. R. (2008) Shewanella secretes flavins that mediate extracellular electron transfer. *Proc. Natl. Acad. Sci. USA* **105**, 3968–3973.

Mikutta C. and Kretzschmar R. (2008) Synthetic coprecipitates of exopolysaccharides and ferrihydrite. Part II: Siderophore-promoted dissolution. *Geochim. Cosmochim. Acta* **72**, 1128–1142.

Mikutta C., Mikutta R., Bonneville S., Wagner F., Voegelin A., Christl I. and Kretzschmar R. (2008) Synthetic coprecipitates of exopolysaccharides and ferrihydrite. Part I: Characterization. *Geochim. Cosmochim. Acta* **72**, 1111–1127.

Myers C. R. and Myers J. M. (1994) Ferric iron reduction-linked growth yields of Shewanella putrefaciens MR-1. *J. App. Bact.* **76**, 253–258.

Nealson K. H. and Myers C. R. (1990) Iron reduction by bacteria - a potential role in the genesis of Banded Iron Formations. *Am. J. Sci.* **290A**, 35–45.

Nevin K. P. and Lovley D. R. (2002a) Mechanisms for Fe(III) oxide reduction in sedimentary Environments. *Geomicrobiol. J.* **19**, 141–159.

Nevin K. P. and Lovley D. R. (2002b) Mechanisms for accessing insoluble Fe(III) oxide during dissimilatory Fe(III) reduction by Geothrix fermentans. *Appl. Environ. Microbiol.* **68**, 2294–2299.

O'Loughlin E. J. (2008) Effects of electron transfer mediators on the bioreduction of lepidocrocite (γ-FeOOH) by Shewanella putrefaciens CN32. *Environ. Sci. Technol.* **42**, 6876–6882.

Piepenbrock A., Dippon U., Porsch K., Appel E. and Kappler A. (2011) Dependence of microbial magnetite formation on humic substance and ferrihydrite concentrations and Fe(II):Fe(total) ratio. *Geochim. Cosmochim. Acta* **75**, 6844–6858.

Raven K. P., Jain A. and Loeppert R. H. (1998) Arsenite and arsenate adsorption on ferrihydrite: kinetics, equilibrium, and adsorption envelopes. *Environ. Sci. Technol.* **32**, 344–349.

Reguera G., McCarthy K. D., Mehta T., Nicoll J. S., Tuominen M. T. and Lovley D. R. (2005) Extracellular electron transfer via microbial nanowires. *Nature* **435**, 1098–1101.

Roden E. E. (2003) Fe(III) Oxide reactivity toward biological versus chemical reduction. *Environ. Sci. Technol.* **37**, 1319–1324.

Roden E. E. and Zachara J. M. (1996) Microbial reduction of crystalline iron(III) oxides: influence of oxide surface area and potential for cell growth. *Environ. Sci. Technol.* **30**, 1618–1628.

Roden E. E., Kappler A., Bauer I., Jiang J., Paul A., Stoesser R., Konishi H. and Xu H. (2010) Extracellular electron transfer through microbial reduction of solid phase humic substances. *Nat. Geosci.* **3**, 417–421.

Royer R. A., Burgos W. D., Fisher A. S., Unz R. F. and Dempsey B. A. (2002a) Enhancement of biological reduction of hematite by electron shuttling and Fe(II) complexation. *Environ. Sci. Technol.* **36**, 1939–1946.

Royer R. A., Burgos W. D., Fisher A. S., Jeon B. H., Unz R. F. and Dempsey B. A. (2002b) Enhancement of hematite bioreduction by natural organic matter. *Environ. Sci. Technol.* **36**, 2897–2904.

Ruebush S. S., Brantley S. L. and Tien M. (2006) Reduction of soluble and insoluble iron forms by membrane fractions of Shewanella oneidensis grown under aerobic and anaerobic conditions. *Appl. Environ. Microbiol.* **72**, 2925–2935.

Schwertmann U. and Cornell R. M. (2000) *Iron Oxides in the Laboratory*. Wiley-VCH Verlag GmbH, Weinheim.

Sharma P., Ofner J. and Kappler A. (2010) Formation of binary and ternary colloids and dissolved complexes of organic matter, Fe and As. *Environ. Sci. Technol.* **44**, 4479–4485.

Stevenson F. J. (1994) *Humus Chemistry – Genesis, Composition*. Reactions. John Wiley & Sons, Inc., New York.

Stookey L. L. (1970) Ferrozine – a new spectrophotometric reagent for iron. *Anal. Chem.* **42**, 779–781.

Taillefert M., Beckler J. S., Carey E., Burns J. L., Fennessey C. M. and DiChristina T. J. (2007) Shewanella putrefaciens produces an Fe(III)-solubilizing organic ligand during anaerobic respiration on insoluble Fe(III) oxides. *J. Inorg. Biochem.* **101**, 1760–1767.

Thamdrup B. (2000) Bacterial manganese and iron reduction in aquatic sediments. In *Adv. Microb. Ecol.* (ed. B. Schink). Kluwer Academic/Plenum Publishers, New York.

Thieme J., McNulty I., Vogt S. and Paterson D. (2007) X-ray spectromicroscopy – A tool for environmental sciences. *Environ. Sci. Technol.* **41**, 6885–6889.

Venkateswaran K., Moser D. P., Dollhopf M. E., Lies D. P., Saffarini D. A., MacGregor B. J., Ringelberg D. B., White D. C., Nishijima M., Sano H., Burghardt J., Stackebrandt E. and Nealson K. H. (1999) Polyphasic taxonomy of the genus Shewanella and description of Shewanella oneidensis sp. nov. *Int. J. Syst. Bacteriol.* **49**, 705–724.

Vermeer A. W. P., van Riemsdijk W. H. and Koopal L. K. (1998) Adsorption of humic acid to mineral particles. 1. specific and electrostatic interactions. *Langmuir* **14**, 2810–2819.

Voillier E., Inglett P. W. K. H., Roychoudhury A. N. and Van Cappellen P. (2000) The ferrozine method revisited: Fe(II)/Fe(III) determination in natural waters. *Appl. Geochem.* **15**, 785–790.

von Canstein H., Ogawa J., Shimizu S. and Lloyd J. R. (2008) Secretion of flavins by Shewanella species and their role in extracellular electron transfer. *Appl. Environ. Microbiol.* **74**, 615–623.

Weber K. A., Achenbach L. A. and Coates J. D. (2006) Microorganisms pumping iron: anaerobic microbial iron oxidation and reduction. *Nat. Rev. Microbiol.* **4**, 752–764.

Weng L. P., van Riemsdijk W. H., Koopal L. K. and Hiemstra T. (2006) Adsorption of humic substances on goethite: Comparison between humic acids and fulvic acids. *Environ. Sci. Technol.* **40**, 7494–7500.

Wolf M., Kappler A., Jiang J. and Meckenstock R. U. (2009) Effects of umic substances and quinones at low concentrations on ferrihydrite reduction by Geobacter metallireducens. *Environ. Sci. Technol.* **43**, 5679–5685.

Zachara J. M., Kukkadapu R. K., Fredrickson J. K., Gorby Y. A. and Smith S. C. (2002) Biomineralization of poorly crystalline Fe(III) oxides by dissimilatory metal reducing bacteria (DMRB). *Geomicrobiol. J.* **19**, 179–207.

Associate editor: Stephan Kraemer